文章编号: 1001 - 9014(2015)02 - 0140 - 05　　DOI: 10.11972/j.issn.1001 - 9014.2015.02.003

A direction finding technique using millimeter wave interferometer

WANG Lan-Mei[1], LIN Ji-Ping[1], WANG Gui-Bao[2*], CHEN Zhi-Hai[1]

(1. School of Physics and Optoelectronic Engineering, Xidian University, Xi'an 710071, China
2. School of Physics and Telecommunication Engineering, Shanxi University of Technology, Hanzhong 723001, China)

Abstract: A two-dimensional direction finding ambiguity resolution algorithm about millimeter wave interferometer is proposed in the paper. By means of implementing one or more times virtual transformation operation on measured phase differences between the original circular array elements and the reference array element, the unambiguous phase differences between the virtual array element and reference array element are achieved. The unambiguous phase differences are used to give rough but unambiguous estimation of direction of arrival (DOA), which are used as coarse references to disambiguate the cyclic phase ambiguities in phase differences between the original array element and the reference array element. The high-precision estimations of DOA are acquired. Simulation examples have verified that the algorithm can obtain the two-dimensional direction finding results with high accuracy in the millimeter wave frequency range.

Key words: array signal processing, millimetre wave, interferometer, direction finding, ambiguity resolution, uniform circular array

PACS: 84.40.-x, 41.20.Jb, 84.40.Ua

一种毫米波干涉仪测向算法

王兰美[1]， 林吉平[1]， 王桂宝[2*]， 陈智海[1]

(1. 西安电子科技大学 物理与光电工程学院,陕西 西安　710071;
2. 陕西理工学院 物理与电信工程学院,陕西 汉中　723001)

摘要:提出了一种毫米波干涉仪二维测向解模糊算法.通过对圆形阵列阵元与参考阵元之间的测量相位差进行一次或多次虚拟变换运算,获得虚拟阵元与参考阵元之间的无模糊相位差.无模糊相位差被用来得到粗略无模糊的波达方向估计,此粗略无模糊的波达方向估计被用来解原阵列阵元和参考阵元的周期性相位模糊.进而获得高精度波达方向估计.仿真实验表明,所提算法在毫米波频率范围内能获得高精度的二维测向结果.

关　键　词:阵列信号处理;毫米波;干涉仪;测向;解模糊;均匀圆阵

中图分类号:TN911.23　　**文献标识码**:A

Introduction

With recent advances in millimeter wave technology, including the availability of high-power sources in this band, the millimeter waves are widely applied in the military and commercial applications[1-3]. The interferometer direction finding is used to determine the direction of arrival (DOA) by directly or indirectly measuring the phase differences among the antenna induced signal distributed in different spatial position[4-5]. Millimeter wave interferometer direction finding has the advantages of both millimeter wave and interferometer direction finding, which has a wide application in communications, radar, guidance system, radio astronomy and so on.

The phase difference ambiguity resolution is an important technique to promote the performance of millimeter wave interferometer direction finder[6-7]. The long and short baseline methods for resolving ambiguity require that the length of short baseline is less than the minimal

Received date: 2013 - 09 - 19, **revised date**: 2015 - 01 - 27　　**收稿日期**: 2013 - 09 - 19, **修回日期**: 2015 - 01 - 27

Foundation items: Supported by National Natural Science Foundation of China (61201295, 61271300, 61100156, 61402365), and the Fundamental Research Funds for the Central Universities (K5051307017)

Biography: WANG Lan-Mei (1975-), female, Shan Dong, China, PhD. Research fields focus on the polarization sensitive array signal processing and the application of compressed sensing and frame theory in array signal processing. E - mail: lmwang@mail.xidian.edu.cn

* **Corresponding author**: E-mail: gbwangxd@126.com

half wavelength of incident signal[8-9]. For the millimeter wave interferometer direction finder, the wavelength of millimeter wave is extremely short, it is difficult to implement the antenna baseline length that is less than half wavelength in engineering[10]. However, it is required the antenna baseline length that is greater than half wavelength in many application scenarios, thus the phase ambiguities are emerged, the traditional direction finding methods based on long and short baseline are invalid[11-12]. The virtual array transformation algorithm is presented in[13-15], but the DOA estimation requires rough prior information of azimuth and elevation angles.

The purpose of this paper is to solve phase ambiguities in millimeter interferometer direction finding system by using the virtual baseline transform algorithm. The virtual transformation operation on measured phase differences will not cease until the unambiguous phase differences are acquired. The unambiguous phase differences can be used to obtain the actual phase differences of original array.

1 Signal and array models

Consider an M-element uniform circular array (UCA) in the x-y plane with its center at the origin of the Cartesian coordinates and radius of R is greater than half of minimal wavelength of the incident signals. The reference element is located at the origin of the Cartesian coordinates. The first array element located on the cross point of circle and the positive x-axis, along the anti-clockwise direction is respectively the first, second, ..., Mth array element, as shown in Fig. 1.

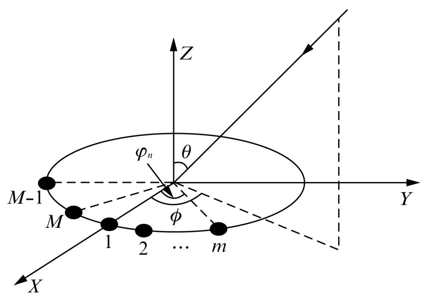

Fig. 1　Uniform circular array geometry
图 1　均匀圆形阵列结构图

Assume that the millimeter wave radar signal having the wavelength λ impinges upon the circular array from the direction of (θ, ϕ), where $\theta \in [0, \pi/2]$ is the signal's elevation angle measured down from the positive z-axis, $\phi \in [0, 2\pi]$ denotes the azimuth angle measured counter-clockwise from the positivex-axis. $\varphi_m = 2\pi(m-1)/M$, $m = 1, \cdots, M$ are the location of array elements.

The phase difference between the mth array element and the reference array element is:

$$\varphi_{0,m} = \frac{2\pi R}{\lambda}\sin\theta\cos(\phi - \varphi_m) \quad \varphi_m = \frac{2\pi(m-1)}{M} . \quad (1)$$

Equation (1) can be rewritten in the following matrix form:

$$\varphi_{0,m} = \frac{2\pi R}{\lambda}[\sin\varphi_m, \cos\varphi_m]\begin{bmatrix}\sin\theta\sin\phi \\ \sin\theta\cos\phi\end{bmatrix} . \quad (2)$$

The actual phase difference vector $\boldsymbol{\Phi} = [\varphi_{01}, \varphi_{02}, \cdots, \varphi_{0M}]^T$ between the M-element UCA and the reference array element are:

$$\boldsymbol{\Phi} = \frac{2\pi R}{\lambda}\boldsymbol{W}\boldsymbol{\Gamma} \quad , \quad (3)$$

where $\boldsymbol{W}$ is the angular position matrix determined by the angular position of the array element, $\boldsymbol{\Gamma}$ is the direction cosine vector determined by the direction cosine of signal. $\boldsymbol{W}$ and $\boldsymbol{\Gamma}$ have the form as:

$$\boldsymbol{W} = \begin{bmatrix} 0 & 1 \\ \sin\left(\frac{2\pi}{M}\right) & \cos\left(\frac{2\pi}{M}\right) \\ \vdots & \vdots \\ \sin\left[(M-1)\frac{2\pi}{M}\right] & \cos\left[(M-1)\frac{2\pi}{M}\right] \end{bmatrix},$$

$$\boldsymbol{\Gamma} = \begin{bmatrix}\sin\theta\sin\phi \\ \sin\theta\cos\phi\end{bmatrix} \quad . \quad (4)$$

Let $\hat{\boldsymbol{\Phi}}$ be the measured phase difference vector between the M-element and the reference array element, respectively, i. e., $\hat{\boldsymbol{\Phi}} = [\hat{\varphi}_{01}, \hat{\varphi}_{02}, \cdots, \hat{\varphi}_{0M}]^T$. When array radius R is greater than half wavelength, namely $R > \frac{\lambda}{2}$, there exists $2\pi\boldsymbol{p}$ deviation between $\hat{\boldsymbol{\Phi}}$ and $\boldsymbol{\Phi}$, their relationship can be expressed as:

$$\boldsymbol{\Phi} = \hat{\boldsymbol{\Phi}} + 2\pi\boldsymbol{p} \quad , \quad (5)$$

where $\boldsymbol{p} = [p_1, p_2, \cdots, p_M]$ is the phase cycle number ambiguity vector. To measure the DOA of signal, it is necessary to determine the phase cycle number ambiguity vector $\boldsymbol{p}$.

2 Virtual transformation algorithm

The virtual transformations are done on the mth and nth array elements, thus the phase difference between the kth virtual array element and the reference array element is obtained:

$$\hat{\varphi}_{0,n} + \hat{\varphi}_{0,m} = \frac{2\pi\left\{2R\cos\left[\frac{\pi}{M}(m-n)\right]\right\}}{\lambda} \sin\theta\cos\left[\phi - \left(\frac{m+n}{2} - 1\right)\cdot\frac{2\pi}{M}\right] \quad . \quad (6)$$

From Eq. 1 and 6, after first time virtual transformation, the virtual radius of circular array is $R^{(1)} = 2R\cos[\pi(m-n)/M]$. The virtual shrinking transformation is not existent unless the following condition is satisfied:

$$0 < R^{(1)} < R \quad . \quad (7)$$

Equation 7 can be rewritten as:

$$0 < 2R\cos\left[\pi\frac{(m-n)}{M}\right] < R \Rightarrow$$

$$0 < \cos\left[\frac{\pi\,|m-n|}{M}\right] < \frac{1}{2} \quad . \quad (8)$$

According to Eq. 8, it can be got that:

$$M/3 < |m-n| < M/2 \quad . \quad (9)$$

When the integers m and n satisfy the Eq. 9, the virtual shirking transformation can be done, the ambiguities are disambiguated.

2.1 Integer times virtual transformation

When $|m-n|$ is even number, namely m and n are both even or odd numbers, $(m+n)/2$ is integer. Let $k = (m+n)/2$, after one time virtual shrinking transformation, the phase difference between the kth ($k = 1, \cdots, M$) virtual array element and the reference array element can be expressed as:

$$\varphi_{0,k}^{(1)} = \hat{\varphi}_{0,n} + \hat{\varphi}_{0,m} = \frac{2\pi R^{(1)}}{\lambda} \sin\theta\cos\left[\phi - (k-1)\cdot\frac{2\pi}{M}\right] \quad . \quad (10)$$

The angular position matrices of virtual and actual circular arrays are the same, but the radii of the two arrays are different, as is shown in Fig. 2.

As an alternative the Eq. 10 can be expressed in matrix notation as follows

$$\boldsymbol{\Phi}^{(1)} = \boldsymbol{T}\hat{\boldsymbol{\Phi}} \quad , \quad (11)$$

where $\boldsymbol{\Phi}^{(1)} = [\varphi_{0,1}^{(1)}, \varphi_{0,2}^{(1)}, \cdots, \varphi_{0,M}^{(1)}]$ is the phase difference vector after the first time virtual transformation, $\hat{\boldsymbol{\Phi}}$ is the measured phase difference vector, $\boldsymbol{T}$ is the virtual transformation matrix determined by the Eq. 10.

If $R^{(1)}$ is still greater than minimal half wavelength, so $\boldsymbol{\Phi}^{(1)}$ still exists phase ambiguity. It can continue do the virtual transformation in accordance with the above method until the radius of the virtual circular array is less than minimal half wavelength.

Suppose that it have conducted L times virtual transformations, furthermore, the radius of virtual circular array, namely $R^{(L)}$ meets the condition as follows:

$$R^{(L)} = R\left[2\cos\frac{\pi(m-n)}{M}\right]^L < \frac{\lambda}{2} \quad , \quad (12)$$

where L is the minimal positive integer that satisfies the Eq. 12, $R^{(L)}$ is the radius of virtual circular array after L times virtual transformations. The relationship between $\boldsymbol{\Phi}^{(L)}$ and $R^{(L)}$ can be expressed as:

$$\boldsymbol{\Phi}^{(L)} = \frac{2\pi R^{(L)}}{\lambda}\boldsymbol{W}\boldsymbol{\Gamma} \quad , \quad (13)$$

where $\boldsymbol{\Phi}^{(L)} = [\varphi_{0,1}^{(L)}, \varphi_{0,2}^{(L)}, \cdots, \varphi_{0,M}^{(L)}]^{\mathrm{T}}$ is the phase difference vector after L times virtual transformation. There is no phase ambiguity in $\boldsymbol{\Phi}^{(L)}$, which means that $\boldsymbol{\Phi}^{(L)}$ can be expressed in algebra notation as follows: $\varphi_{0,k}^{(L)} \in [-\pi, \pi]$ $1 \leqslant k \leqslant M$. $\boldsymbol{W}$ and $\boldsymbol{\Gamma}$ are defined in Eq. 4.

From the analysis above, the relation between $\boldsymbol{\Phi}^{(\mathrm{L})}$ and $\boldsymbol{T}$ can be shown as:

$$\boldsymbol{\Phi}^{(L)} = \boldsymbol{T}^L\hat{\boldsymbol{\Phi}} \quad . \quad (14)$$

2.2 Even number times virtual transformation

When $|m-n|$ is odd number, namely one of m and n is even number and another is odd number, then $(m+n)/2$ in Eq. 6 is not integer. We define the serial number of the virtual array as $d' = (m+n+1)/2$, after the first time virtual shrinking transformation, the phase difference between the d'th virtual array element and the reference array element can be expressed as:

$$\varphi_{0,d'}^{(1)} = \hat{\varphi}_{0,n} + \hat{\varphi}_{0,m} = \frac{2\pi R^{(1)}}{\lambda} \sin\theta\cos\left[\phi - \left(d' - \frac{1}{2}\right)\cdot\frac{2\pi}{M}\right] \quad . \quad (15)$$

From Eq. 15, the angular position matrix of virtual circular array, namely $\boldsymbol{W}_1$ is obtained:

$$\boldsymbol{W}_1 = \begin{bmatrix} \sin\left(\frac{\pi}{M}\right) & \cos\left(\frac{\pi}{M}\right) \\ \sin\left(\frac{3\pi}{M}\right) & \cos\left(\frac{3\pi}{M}\right) \\ \vdots & \vdots \\ \sin\left[(2M-1)\frac{\pi}{M}\right] & \cos\left[(2M-1)\frac{\pi}{M}\right] \end{bmatrix} . \quad (16)$$

From the Eqs. 4 and 16, it can be seen that $\boldsymbol{W}_1$ is completely different from $\boldsymbol{W}$, as is demonstrated in Fig. 3.

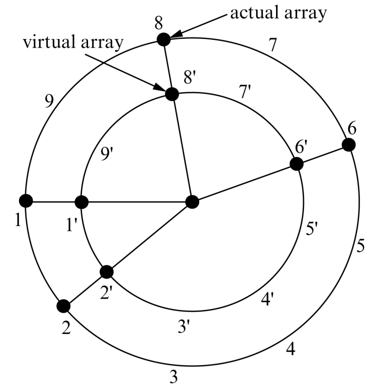

Fig. 2 Uniform circular array with 9 elements
图 2 九元均匀圆形阵列

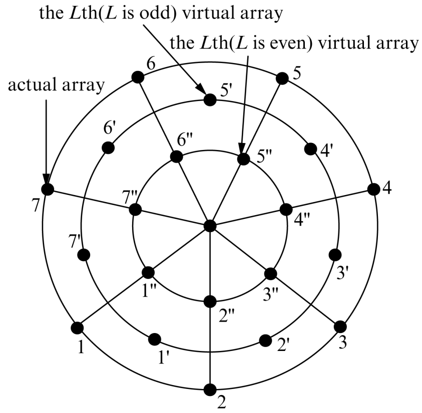

Fig. 3 Uniform circular array with 7 elements
图 3 七元均匀圆形阵列

Equations 15 can also be expressed in matrix notation as follows

$$\boldsymbol{\Phi}^{(1)} = \boldsymbol{T}_1\hat{\boldsymbol{\Phi}} \quad , \quad (17)$$

where $\boldsymbol{T}_1$ is the first time virtual transformation matrix determined by the Eq. 15, $\boldsymbol{\Phi}^{(1)}$ is the phase difference vector after the first time virtual transformation. In view of the above condition, the angular position matrix is different in before and after the first time virtual transformation. Even if $R^{(1)}$ is less than minimal half wavelength, it is hard to disambiguate the cyclic phase ambiguities. After the second time virtual shrinking transformation, the phase differences are represented as:

$$\varphi_{0,d''}^{(2)} = \hat{\varphi}_{0,n'}^{(1)} + \hat{\varphi}_{0,m'}^{(1)} = \frac{2\pi R^{(2)}}{\lambda} \sin\theta\cos\left[\phi - (d''-1)\cdot\frac{2\pi}{M}\right] \quad , \quad (18)$$

where $M/3 < |m'-n'| < M/2$, $|m'-n'|$ is odd number, then $d'' = \frac{m'+n'-1}{2}$ is integer. From the above analysis, the formulas (18) and (10) have the same form.

Equation 18 can also be expressed in matrix notation as follows

$$\boldsymbol{\Phi}^{(2)} = \boldsymbol{T}_2\boldsymbol{\Phi}^{(1)} \quad , \quad (19)$$

where $\boldsymbol{T}_2$ is the second time virtual transformation matrix determined by the Eq. 18, $\boldsymbol{\Phi}^{(2)}$ is the phase difference vector after the second time virtual transformation.

When two times virtual transformations have been done, the angular position matrix is the same before and after the two times virtual transformation. As a result, it needs even number time virtual shrinking transformation to disambiguate the cyclic phase ambiguities. According to Eqs. 17 and 19, the first time virtual transformation matrix $\boldsymbol{T}_1$ and the second time virtual transformation matrix $\boldsymbol{T}_2$ are obtained. Suppose $\boldsymbol{\Phi}^{(L)}$ is the phase difference vector after L times virtual transformations, then the relationship between $\boldsymbol{\Phi}^{(L)}$ and $\hat{\boldsymbol{\Phi}}$ can be expressed as follows:

$$\boldsymbol{\Phi}^{(L)} = (\boldsymbol{T}_2\boldsymbol{T}_1)^{\frac{L}{2}}\hat{\boldsymbol{\Phi}} \quad , \quad (20)$$

where L is the minimal positive even number that meets Eq. 12, $\hat{\boldsymbol{\Phi}}$ is the original measured phase difference vector.

2.3 Virtual transformation to disambiguate the cyclic phase ambiguities

The problem at hand is formulated in terms of the theory of interferometer direction finder technology, the rough but unambiguous estimates of the actual phase difference vector $\overline{\boldsymbol{\Phi}}$ can be expressed as

$$\overline{\boldsymbol{\Phi}} = \frac{R}{R^{(L)}}\boldsymbol{\Phi}^{(L)} \quad . \quad (21)$$

From Eqs. 5 and 21, the phase cycle number ambiguity vector $\boldsymbol{p}_{\text{opt}}$ is got:

$$\boldsymbol{p}_{\text{opt}} = \arg\min|\overline{\boldsymbol{\Phi}} - (\hat{\boldsymbol{\Phi}} + 2\pi p)| \quad . \quad (22)$$

Then the high-precision estimations of actual phase difference vector $\tilde{\boldsymbol{\Phi}}$ can be acquired as:

$$\tilde{\boldsymbol{\Phi}} = \hat{\boldsymbol{\Phi}} + 2\pi\boldsymbol{p}_{\text{opt}} \quad . \quad (23)$$

From Eqs. 3 and 23, it can be obtained that:

$$\tilde{\boldsymbol{\Phi}} = \boldsymbol{E}\tilde{\boldsymbol{\Gamma}} \quad , \quad (24)$$

where

$$\boldsymbol{E} = \frac{2\pi R}{\lambda}\boldsymbol{W} \quad \tilde{\boldsymbol{\Gamma}} = \begin{bmatrix}\tilde{\Gamma}_1\\ \tilde{\Gamma}_2\end{bmatrix} = \begin{bmatrix}\sin\tilde{\theta}\sin\tilde{\phi}\\ \sin\tilde{\theta}\cos\tilde{\phi}\end{bmatrix}$$

Based on the least square method, the accurate estimation value of direction cosine is obtained:

$$\tilde{\boldsymbol{\Gamma}} = \begin{bmatrix}\tilde{\Gamma}_1\\ \tilde{\Gamma}_2\end{bmatrix} = \begin{bmatrix}\sin\tilde{\theta}\sin\tilde{\phi}\\ \sin\tilde{\theta}\cos\tilde{\phi}\end{bmatrix} = \boldsymbol{E}^{\#}\boldsymbol{\Phi} \quad , \quad (25)$$

where $\boldsymbol{E}^{\#} = (\boldsymbol{E}^H\boldsymbol{E})^{-1}\boldsymbol{E}^H$ is pseudo inverse matrix of $\boldsymbol{E}$.

From Eq. 25, the accurate estimation value of azimuth and elevation are got:

$$\begin{cases}\tilde{\theta} = \arcsin\sqrt{\tilde{\Gamma}_1^2 + \tilde{\Gamma}_2^2}\\ \begin{cases}\tilde{\phi} = \arctan\left(\dfrac{\tilde{\Gamma}_1}{\tilde{\Gamma}_2}\right), \tilde{\Gamma}_2 \geq 0\\ \tilde{\phi} = \pi + \arctan\left(\dfrac{\tilde{\Gamma}_1}{\tilde{\Gamma}_2}\right), \tilde{\Gamma}_2 < 0\end{cases}\end{cases} \quad . \quad (26)$$

Thus the two-dimensional angle estimation with high precision is obtained while the direction finding ambiguity is resolved.

3 Simulation results

In this section, some simulations are conducted to evaluate the performances on DOA estimation by the proposed method. The single-frequency signal with parameter $\theta = 30°$, $\phi = 43°$ impinging upon a 9-element uniform circular array with a radius of $R = 3.5\lambda$, as shown in Fig. 2. The carrier frequency is 60 GHz, or equivalently, with wavelength $\lambda = 5$ mm. 512 snapshots are used in each of the 500 independent Monte Carlo simulation experiments, and the scatter diagram is simulated at SNR = 15 dB.

From Fig. 5, it is shown that almost all estimated values are located in the vicinity of actual value after virtual transformation, the estimated value of $\hat{\theta}$ and $\hat{\phi}$ range from the numerical range (29.98°, 30.03°) and (42.97°, 43.03°), respectively. On the contrary, before virtual transformation the estimated values are wrongly distributed in the range of the azimuth (−3.5°, −4.5°) and the elevation (2.12°, 2.17°).

Figures 6 – 7 show that the RMSE of elevation and azimuth before virtual transformation are 27.85° and 47°. But the RMSE of elevation and azimuth after virtual

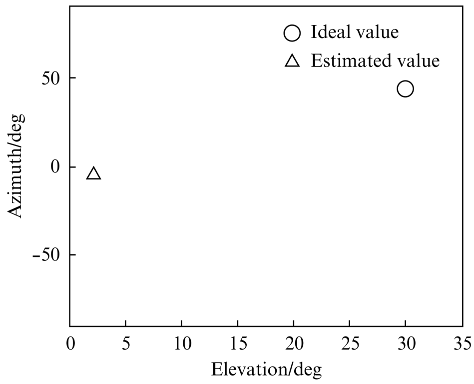

Fig. 4 Scatter diagram before virtual transformation
图 4 虚拟变换前的散布图

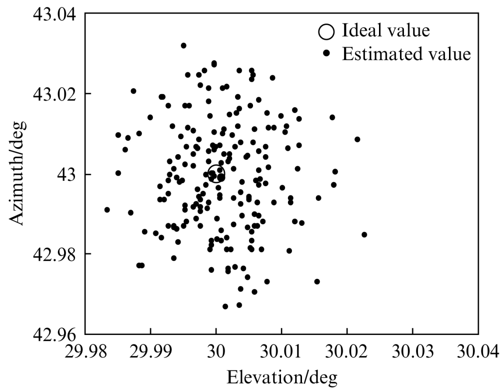

Fig. 5 Scatter diagram after virtual transformation
图 5 虚拟变换后的散布图

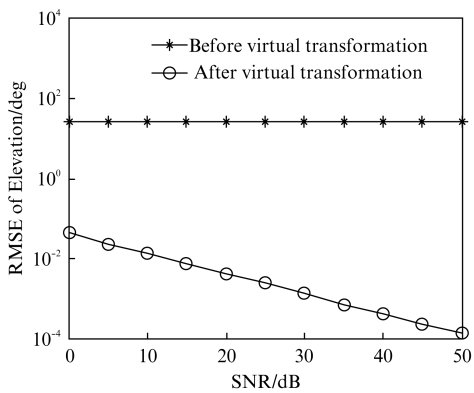

Fig. 6 RMSE of elevation versus SNR
图 6 俯仰角均方根误差随信噪比关系

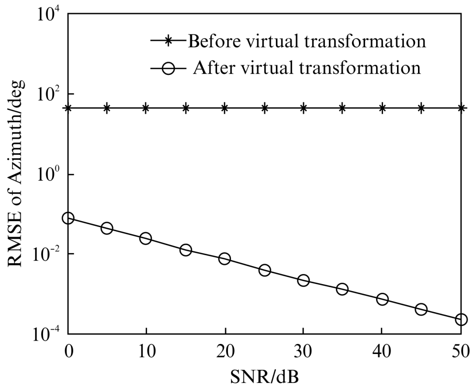

Fig. 7 RMSE of azimuth versus SNR
图7 方位角均方根误差随信噪比关系

transformation are reduced evidently as the SNR increases, which are less than 0.045° and 0.08° in the SNR range. The virtual transform can effectively solve the problem of phase ambiguities, hence the precise estimates of DOA can be obtained.

In order to further validate the feasibility of the proposed method, the UCA method, the uniform concentric circular array (UCCA) method and the proposed method of this paper are compared in Fig. 8. Without loss of generality, nine array elements are placed on each circular

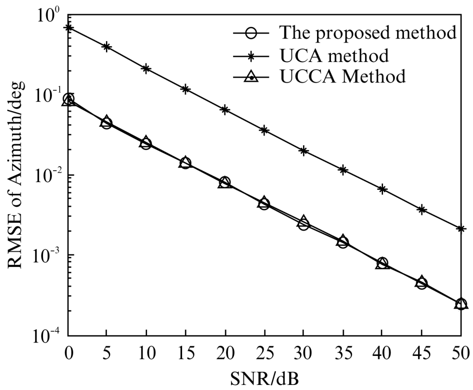

Fig. 8 RMSE of azimuth versus SNR
图8 方位角均方根误差随信噪比关系

ring. Suppose the radius of UCA is $R_U = 0.4222\lambda$, which doesn't exist phase ambiguities. The inner and outer radius of UCCA are $R_1 = 3.5\lambda$ and $R_2 = 0.4222\lambda$ respectively. The radius of this proposed method before and after two times virtual transformation are $R = 3.5\lambda$ and $R^{(2)} = 0.4222\lambda$.

The curves with star, triangle and circular points in Fig. 8 plot the RMSE of azimuth estimated by the UCA method, UCCA method and the proposed method, respectively, at different SNR levels. In the SNR range (namely, at or above 0 dB) the azimuth estimation precision based on the UCA model is lower than that of the UCCA method and the proposed method. The proposed method is nearly the same as UCCA method versus SNR. The proposed method and UCCA method can overcome DOA ambiguities by virtual baseline transformation and long-short baselines, respectively. But the number of array element is $9 \times 2 = 18$ for UCCA method and 9 for the proposed method. Alternatively, the simulation and discussion for the elevation are similar to the azimuth.

4 Conclusions

A virtual transformation method for two-dimensional direction finding about millimeter wave interferometer has been researched. In a first step the unambiguous phase difference vector is obtained by means of implementing L times virtual transformations. In a second step the actual array phase difference vector is acquired by disambiguating the cyclic phase ambiguities. The proposed algorithm not only overcomes the weakness of the ambiguity of DOA estimation of sparse arrays, but also improves the capability of resolution. Numerical examples illustrate the performance of the proposed techniques, which is much better than UCA method and nearly the same as UCCA method.

References

[1] Kim S, Nguyen C. A displacement measurement technique using millimeter-wave interferometry[J]. *IEEE Transactions on Microwave Theory and Techniques*, 2003, **51**(6): 1724-1728.

[2] Choi M S, Grosskopf G, Rohde D, *et al*. Experiments on DOA-estimation and beamforming for 60 GHz smart antennas[C]. *In the 57th IEEE Semiannual Vehicular Technology Conference*, Jeju, South Korea, 2003: 379-387.

[3] Liu B, Pan Z H, Li D J, *et al*. Moving target detection and location based on millimeter wave InISAR imaging[J]. *J. Infrared Millim. Waves*, 2012, **31**(3): 258-264.

[4] Wei H W, Shi Y G. Performance analysis and comparison of correlative interferometers for direction finding[C]. *In IEEE 10th International Conference on Signal Processing (ICSP)*, Beijing, China, 2010: 393-396.

[5] Lim J S, Jung C G, Chae G S. A design of precision RF direction finding device using circular interferometer[C]. *In Proceedings of International Symposium on Intelligent Signal Processing and Communication Systems*, Seoul, Korea, 2004: 713-716.

[6] Wang L M, Wang G B, Chen Z H. Joint DOA-polarization estimation based on uniform concentric circular array[J]. *Journal of Electromagnetic Waves and Applications*, 2013, **27**(13): 1702-1714.

[7] Gavish M, Weiss A J. Array geometry for ambiguity resolution in direction finding[J]. *IEEE Transactions on Antennas and Propagation*, 1996, **44**(6): 889-895.

[8] Wu Y W, Rhodes S, Satorius E H. Direction of arrival estimation via extended phase interferometry[J]. *IEEE Transactions on Aerospace and Electronic Systems*, 1995, **31**(1): 375-381.

[9] Wong K T, Zoltowski M. D. Direction finding with sparse rectangular dual-size spatial invariance array[J]. *IEEE Transactions on Aerospace and Electronic Systems*, 1998, **34**(4): 1320-1327.

[10] Pan Z H, Liu B, Zhang Q J. Millimeter-wave InSAR phase unwrapping and DEM reconstruction based on three-baseline[J]. *J. Infrared Millim. Waves*, 2013, **32**(5): 474-480.

[11] Jacobs E, Ralston E E. Ambiguity resolution in interferometry[J]. *IEEE Transactions on Aerospace and Electronic Systems*, 1981, AES-17(4): 766-779.

[12] Zhou Y Q, Huang F K. Solving ambiguity problem of digitized multi-baseline interferometer under noisy circumstance[J]. *Journal of China Institute of Communications*, 2005, **34**(8): 16-21.

[13] Wang Y L, Chen H, Wan S H. An effective DOA method via virtual array transformation[J]. *Science in China*, *Series. E*, 2001, **44**(1): 75-82.

[14] Kim Y S, Kim Y S. Improve resolution capability via virtual expansion of array[J]. *Electronics. Letters*, 1999, **35**(19): 1596-1597.

[15] Heung H Y, Kim Y S, Kim C J. Spatially close signals separation via array aperture expansions and spatial spectrum averaging[J]. *ETRI Journal*, 2004, **26**(1): 45-47.